Supporting information

Evaluation of the Effects of G4 Ligands on the Interaction between G-Quadruplexes and Their Binding Proteins

Yuma Tanaya,[a] Manaho Sashida,[a] Hisao Masai,[b] Hiroyuki Sasanuma,[b] Daimei Miura,[a] Ryutaro Asano,[a] Kazuo Nagasawa[a] and Masayuki Tera*[a]

[a] Department of Biotechnology and Life Science, Tokyo University of Agriculture and Technology, Naka-cho, Koganei city, Tokyo 184-8588, Japan E-mail: tera@go.tuat.ac.jp
[b] Department of Basic Medical Sciences, Tokyo Metropolitan Institute of Medical Science, Kamikitazawa, Setagaya-ku, Tokyo, 156-8506, Japan.

Table of contents

General information 2
Experimental methods 3
Supplementary Table S1 7
Supplementary Table S2 7
Supplementary Figure S1. 8
Supplementary Figure S2. 9
Supplementary Figure S3. 9
Supplementary Figure S4. 10
Supplementary Figure S5. 10
Supplementary Figure S6. 11
Supplementary Figure S7. 11
Supplementary Figure S8. 12
Supplementary Figure S9. 12
Supplementary Figure S10. 13
Supplementary Figure S11. 13
Synthetic procedures 14
NMR spectra 17
References 22

General information

Materials and Analytical Methods

All chemicals and reagents were purchased from Sigma-Aldrich, Wako Chemicals, or TCI unless otherwise noted. Flash column chromatography was performed using either Silica Gel 60 (spherical, particle size 40–100 μm; Kanto Chemical, Cat. #37559-85) or NH Silica Gel (spherical, particle size 100 μm; Fuji Silysia, Cat. #NH-DM1020). Reversed-phase chromatography was conducted using an EPCLC-AI-580S instrument (YAMAZEN CORPORATION). Chromatographic separation was achieved on a UNIVERSAL™ Premium-ODS (Φ2.3 × 12.3 cm, 30 μm; YAMAZEN CORPORATION, Cat. #UW212). The mobile phase consisted of H_2O (solvent A) and acetonitrile (solvent B), and a stepwise gradient elution was applied from 92% solvent A to 63% solvent B over 33 minutes. The flow rate was set at 10 mL/min, and UV detection was performed at 254 nm. Analytical HPLC data were acquired using a ChromNAV system. Separation was performed on a CAPCELL PAK C18 MGII (Φ4.6 × 50 mm, 5 μm; 1.0 mL/min, room temperature; OSAKA SODA, Cat. #92529). The mobile phase consisted of 0.1% TFA in H_2O (solvent A) and 0.1% TFA in acetonitrile (solvent B). A stepwise gradient was applied from 80% solvent A to 75% solvent B over 7.5 minutes. Sample injection volumes were 10 μL. ^{1}H and ^{13}C NMR spectra were recorded on a JNM-ECA 500 spectrometer. The spectra are referenced internally according to residual solvent signal of DMSO-d_6 (^{1}H NMR: δ = 2.50 ppm, ^{13}C NMR: δ = 39.52 ppm). The NMR data were recorded as follows: chemical shift (δ, ppm), multiplicity (s = singlet; d = doublet; t = triplet; q = quartet; quint = quintet; m = multiplet; br = broad), integration, and coupling constant (Hz). Data for ^{13}C NMR are reported in terms of chemical shift (δ, ppm). Mass spectra were recorded on a JEOL JMST100X spectrometer with ESI-MS mode using methanol as solvent.

Stock Solutions and Buffers

Stock solutions of **1**–**3** were prepared by dissolving the compounds in DMSO (10 mM). Further dilutions were made from these stock solutions. All experiments were conducted with a final DMSO concentration of < 2.0%. Buffers used in this study were described as below.
Coating buffer: 20 mM phosphate buffer (pH 7.0) containing 70 mM KCl and 0.1% Tween-20.
Wash buffer: 20 mM phosphate buffer (pH 7.0) containing 70 mM KCl and 0.1% Tween-20.
Oligonucleotides were purchased from Eurofins (Japan) and used without further purification.

Sodium dodecyl sulfate-polyacrylamide gel electrophoresis (SDS-PAGE)

SDS-PAGE analysis was carried out with Mini-Protean Gel system (Bio-Rad, USA). PAGE images were acquired on ChemiDoc XRS (Bio-Rad, USA). Image analysis was performed using ImageJ 1.47c (National Institutes of Health, USA).

Experimental methods

Design and Construction of Plasmids

The G4P expression vector used in this study was kindly provided by the Tokyo Metropolitan Institute of Medical Science. The SNAP-tag sequence was designed based on a DNA sequence also provided by the same institute. For BG4, the amino acid sequence of the linker connecting the VH and VL domains was optimized, and the coding sequence was codon-optimized for *E. coli* expression and synthesized by Eurofins. Similarly, the SG4 sequence was codon-optimized for *E. coli* and synthesized by Eurofins. PCR amplification was performed using Phusion® High-Fidelity DNA Polymerase (NEB, Cat. #M0530S). The expression plasmids for BG4, SG4, and SNAP-tag were constructed using the In-Fusion® Snap Assembly Master Mix (Takara Bio, Cat. #Z8947N). Each construct was cloned into either a T7 promoter–based vector or a pET28b vector backbone.[1] All plasmids were verified to be mutation-free by DNA sequencing.

Recombinant Protein Productions

All recombinant proteins were expressed in BL21 (DE3) cells (Nippon Gene, Cat. #312-06534). BG4 expression was carried out based on the previously reported method by D. Miura *et al*[2]. Colonies were first grown overnight at 28 °C in Luria–Bertani (LB) broth supplemented with 50 μg/mL carbenicillin. For protein expression via autoinduction, transformants were then cultured at 20 °C and 170 rpm for 40 h in LB medium containing 0.5% glycerol, 0.05% glucose, 0.2% β-lactose, 50 mM KH_2PO_4, 25 mM $(NH_4)_2SO_4$, 50 mM Na_2HPO_4, 1 mM $MgSO_4$, and 50 μg/mL carbenicillin[3]. After cultivation, the culture supernatant was subjected to ammonium sulfate precipitation (60% w/v) and incubated overnight at 4 °C. The resulting protein precipitates were collected by centrifugation at 4,800 × *g* for 20 min at 4 °C, dissolved in 20 mM potassium phosphate buffer (pH 7.0), and dialyzed overnight against the same buffer at 4 °C. Each recombinant protein was purified using Pierce™ High Capacity Ni-IMAC Resin, EDTA-compatible (Thermo Scientific™, Cat. #A50586), followed by size-exclusion chromatography using a Superdex® 200 Increase 10/300 GL column (Sigma-Aldrich, Cat. #GE28-9909-44) in 20 mM phosphate buffer (pH 7.0) containing 500 mM NaCl.

For SG4, expression was performed in the same manner as for BG4. The resulting recombinant protein was purified using Ni-NTA Agarose (FUJIFILM Wako, Cat. #141-09764), dialyzed overnight against PBS at 4 °C, and concentrated using a Centrifugal Filter Unit (Merck, Cat. #UFC903024).

Expression vectors for G4P and SNAP were transformed into BL21 (DE3) cells. The cells were cultured in LB medium supplemented with 50 μg/mL kanamycin at 37 °C until the optical density at 600 nm (OD_{600}) reached 0.4. Protein expression was induced by the addition of

isopropyl β-D-1-thiogalactopyranoside (IPTG; final concentration, 1.0 mM), followed by incubation at 37 °C for 4 h. After induction, the cells were harvested by centrifugation. Each recombinant protein was purified using Ni-NTA Agarose, dialyzed overnight against PBS at 4 °C, and concentrated using a Centrifugal Filter Unit. Protein concentrations were determined using the BCA Protein Assay Kit (Takara Bio, Cat. #T9300A).

Fluorescence Polarization (FP) Measurements

FP measurements were performed using a multifunctional microplate reader (TECAN, Switzerland, Zurich) with a non-binding 384-well microplate (Greiner, Cat. #781900), employing 40 μL of assay solution per well. The excitation and emission wavelengths were set at 485 nm and 535 nm, respectively. FP values were calculated using the following equation[4–6]:

$$\mathrm{FP\ (mP)} = 1000 \times \frac{\mathrm{S} - \mathrm{G} \times \mathrm{P}}{\mathrm{S} + \mathrm{G} \times \mathrm{P}}$$

where S is the parallel emission intensity, P is the perpendicular emission intensity, and G is the grating factor. The G factor was set to 1.0.

Fluorescent Probe-Based Assay of SNAP-tag Reactivity

Purified SNAP-tag protein (1.0 μM) was incubated with compound **3** (0.2 μM) in 20 mM potassium phosphate buffer (pH 7.0) containing 70 mM KCl, 1 mM DTT, 0.8 mg/mL BSA, 0.2% Tween-20, and 0.2% DMSO. Fluorescence polarization (FP) measurements were performed concurrently during incubation at room temperature for 1 h using excitation/emission wavelengths of 485/535 nm. Following the reaction, 20 μL of each sample was applied to a 12% polyacrylamide gel and subjected to SDS-PAGE under electrophoresis conditions of 80 V for 20 min, followed by 200 V for 35 min. Gels were then imaged using a ChemiDoc™ XRS imaging system.

Circular Dichroism (CD) Spectrometry

CD spectra were recorded using a J-720 spectropolarimeter (JASCO, Japan) equipped with a 10 mm path-length quartz cell. Measurements were performed at room temperature over a wavelength range of 220–320 nm, with a scanning speed of 500 nm/min and a response time of 1 second. Each spectrum represents the average of ten scans. Oligonucleotides (10 μM) were annealed by heating at 95°C for 5 minutes, followed by slow cooling to room temperature in 20 mM potassium phosphate buffer (pH 7.0) containing 70 mM KCl, and 1 mM EDTA. For analysis, 60 μL of the annealed oligonucleotide solution was mixed with an equal volume of 20 mM phosphate buffer (pH 7.0) containing 70 mM KCl, 1 mM DTT, 0.8 mg/mL BSA, and 0.2% Tween-20. before transfer to the quartz cell for measurement.

Far-UV CD analysis of G4P, BG4, and SG4 was conducted under the following conditions. Spectra were recorded over the wavelength range of 190–260 nm using samples at a concentration of 0.3 mg/mL in PBS (pH 7.4), measured at 20 ºC in a 1 cm pathlength cuvette. The sample volume required for each measurement was 75 μL. Data were collected with a spectral bandwidth and step size of 1 nm, and a scan speed of 500 nm/s. The final spectra represent the average of 20 scans. After measurement, the CD spectrum of the corresponding buffer solution was subtracted from each protein spectrum. The resulting data were then converted to mean residue ellipticity (MRE) using the following equation[7]:

$$\mathrm{MRE} = \frac{\theta_\lambda \times \mathrm{MRW}}{10 \times d \times c}$$

Here θ_λ is the observed ellipticity (degrees) at wavelength λ, d is the path length (cm), and c is the protein concentration (g/mL). The mean residue weights (MRW) used were 108 for G4P, 108 for BG4, and 114 for SG4. Data were smoothed using the Savitzky–Golay function and plotted with GraphPad Prism 9.

FP assay

Oligonucleotides (10 nM) were annealed by heating at 95 °C for 5 min, followed by gradual cooling to room temperature in 20 mM potassium phosphate buffer containing 70 mM KCl (pH 7.0). SNAP-tag protein (1.0 μM) and compound **1** (0.2 μM) were preincubated in a solution containing 20 mM potassium phosphate, 70 mM KCl, 1 mM DTT, 0.8 mg/mL BSA, and 0.2% Tween-20 (pH 7.0) at 4 °C for 1 h to prepare compound **4**. Subsequently, compound **4** was serially diluted to yield final concentrations ranging from 100 nM to 0.15 nM. Next, 20 μL of the annealed oligonucleotide solution was mixed with an equal volume of the compound **4** solution and incubated at room temperature for an additional 2 h prior to measurement. All experiments were independently repeated at least five times. Fluorescence polarization (FP) values were plotted against the log-transformed concentrations of compound **4**. Dissociation constants (K_d) were calculated assuming a one-site binding model using GraphPad Prism 9 after outlier exclusion.[8] The following equation was used for the theoretical fitting:

$$FP_\mathrm{obs} = FP_0 + \frac{\Delta FP \times X}{K_\mathrm{d} + X}$$

Here FP_obs is the observed Fluorescence Polarization (FP) value, FP_0 is the FP value in the absence of protein, ΔFP represents the total change in FP between free and fully bound DNA, K_d is the equilibrium dissociation constant, and X is the concentration of the added ligand. Results are presented as mean ± standard deviation (s.d.).

The FP assay using G4-binding proteins (G4BPs) was conducted under the same conditions as the SNAP-tag assay, with the following modifications: the annealing buffer was replaced with

20 mM potassium phosphate, 70 mM KCl, and 1 mM EDTA (pH 7.0), and a G4P (100 nM–0.15 nM) or BG4 (1000 nM–1.5 nM) solution was used instead of compound **4**. G4P and BG4 were prepared in 20 mM potassium phosphate, 70 mM KCl, 1 mM EDTA, 0.8 mg/mL BSA, and 0.2% Tween-20 (pH 7.0).

Fluorescence quenching assays

Fluorescence quenching assays were performed under the same conditions as the FP assay, with excitation and emission wavelengths set at 485 nm and 535 nm, respectively. Fluorescence quenching efficiency at 535 nm was plotted against the log-transformed concentrations of compound **5**.

Enzyme-linked immunosorbent assay (ELISA)

Purified SNAP-tag protein (3.0 μM) was incubated with compound **1** or **2** (15 μM), or 1% DMSO (vehicle control) in coating buffer at 4 °C for 1 hour. The mixture was then diluted 10-fold, and 50 μL/well was immobilized on a 96-well Immuno-plate (Thermo Fisher, USA, Cat. #442404) by incubation at 4°C for 16 hours. Following removal of the coating buffer, wells were blocked with 200 μL/well of blocking buffer (3% BSA (Wako, Cat. #019-27051) in ELISA buffer) for 1 hour at room temperature. Oligonucleotides (10 nM) were annealed by heating at 95°C for 5 minutes, followed by gradual cooling to room temperature in 20 mM potassium phosphate, 70 mM KCl, and 1 mM EDTA (pH 7.0). A 50 μL reaction mixture was prepared by combining 25 μL of the annealed oligonucleotide solution with 25 μL of buffer containing 20 mM potassium phosphate, 70 mM KCl, 1 mM EDTA, 2% BSA, and 0.2% Tween-20 (pH 7.0). The mixture was then added to each well and incubated at room temperature for 2 hours. After a single wash with ELISA buffer, G4BP (1.0 μM) was added in 20 mM potassium phosphate, 70 mM KCl, 1 mM EDTA, 1% BSA, and 0.1% Tween-20 (pH 7.0) at 50 μL/well, followed by 2 hours incubation at room temperature. After three washes with ELISA buffer, wells were incubated with Anti-DYKDDDDY tag, Monoclonal Antibody, Peroxidase Conjugated (Wako, Cat. #015-22391) at a 1:5000 dilution in ELISA buffer (50 μL/well) for 1 hour at room temperature. Following another three washes with ELISA buffer, HRP substrate (TKR, Cat. #T7104A) was added, and chemiluminescence was detected using a ChemiDoc XRS imaging system.

Supplementary Table S1. Sequences of oligonucleotides and topology for their G-quadruplex structures used in FP assay.

Oligonucleotides	Sequence (5' to 3')	topology
Non G4	**FAM**-GTGAGTGCGCTGTGAGGAGTG	**Non G4 ssDNA**
c-kit1	**FAM**-GGGAGGGCGCTGGGAGGAGGG	**Parallel**
Pu24T	**FAM**-TGAGGGTGGTGAGGGTGGGGAAGG	**Parallel**
bcl2	**FAM**-GGGCGCGGGAGGAATTGGGCGGG	**Hybrid**
HT24	**FAM**-TTGGGTTAGGGTTAGGGTTAGGGA	**Hybrid**
c-kit*	**FAM**-GGCGAGGAGGGGCGTGGCCGGC	**Antiparallel**

FAM = fluorescein

Supplementary Table S2. Sequences of oligonucleotides and topology for their G-quadruplex structures used in sandwich ELISA.

Oligonucleotides	Sequence (5' to 3')	topology
Non G4	GTGAGTGCGCTGTGAGGAGTG	**Non G4 ssDNA**
c-kit1	AGGGAGGGCGCTGGGAGGAGGG	**Parallel**
Pu24T	TGAGGGTGGTGAGGGTGGGGAAGG	**Parallel**
bcl2	GGGCGCGGGAGGAATTGGGCGGG	**Hybrid**
HT24	TTGGGTTAGGGTTAGGGTTAGGGA	**Hybrid**
c-kit*	GGCGAGGAGGGGCGTGGCCGGC	**Antiparallel**

A

MDKDCEMKRTTLDSPLGKLELSGCEQGLHRIIFLGKGTSAADAVEVPAPAAVLGGPEPL
MQATAWLNAYFHQPEAIEEFPVPALHHPVFQQESFTRQVLWKLLKVVKFGEVISYSHLA
ALAGNPAATAAVKTALSGNPVPILIPCHRVVQGDLDVGGYEGGLAVKEWLLAHEGHRLG
KPGLGGTENLYFQGSTMDHHHHHHHH

B

MGSSHHHHHHSSGLVPRGSHMHPGHLKGREIGMWYAKKQGQKNKGTGSGAGTGSGAGTG
SGAHPGHLKGREIGMWYAKKQGQKNKGTGSGADYKDHDGDYKDHDIDYKDDDDK

C

MKYLLPTAAAGLLLLAAQPAMAEVQLVQSGAEVKKPGASVKVSCKASGYTFTSYSISWV
RQAPGQGLEWMGWISAYNGNTSYAQKLQGRVTITADKSTSTAYMELSSLRSEDTAVYYC
AKAGHRSGRYNNWFDPWGQGTLVTVSSAAGGGGSGGGGSGGGGSQSELTQPPSVSVAPG
QTARITCGENNIGSKNVHWYQQKPGQAPVLIIYRGSNRPSGIPERFSGSNSGNTATLTI
SRAQAGDEADYYCQVFDRRSDHPVVFGGGTKLTVLAAAENLYFQSSSGDYKDDDDKTRD
YKDDDDKTRDYKDDDDKTRHHHHHHHH

D

MKYLLPTAAAGLLLLAAQPAMAEVELQASGGGFVQPGGSLRLSCAASGGTSGTYNMGWF
RQAPGKEREFVSAISYRDNMTPYYADSVKGRFTISRDNSKNTVYLQMNSLRAEDTATYY
CARYQGRLRIHQSTYWGQGTQVTVSSAAAENLYFQSSSGDYKDDDDKTRDYKDDDDKTR
DYKDDDDKTRHHHHHHHH

Supplementary Figure S1. Amino acid sequences of G4-binding probes and SNAP-tag fusion. (A) SNAP-tag amino acid sequence. (B) G4P amino acid sequence. A C-terminal 3 x FLAG tag was added for binding with the anti-FLAG antibody. (C) BG4 amino acid sequence. A C-terminal 3 x FLAG tag was added for binding with the anti-FLAG antibody. Regions within the linker connecting the VH and VL domains that were modified for optimization are highlighted in yellow. (D) SG4 amino acid sequence. A C-terminal 3 x FLAG tag was added for binding with the anti-FLAG antibody.

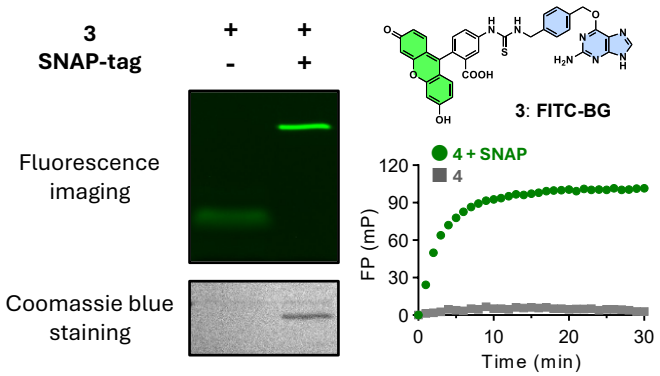

Supplementary Figure S2. Gel analysis (left) and fluorescence polarization assay (right) of SNAP protein with a fluorescently labelled BG derivative (FITC-BG: **3**). The reaction proceeded efficiently within a short time and reached quantitative completion.

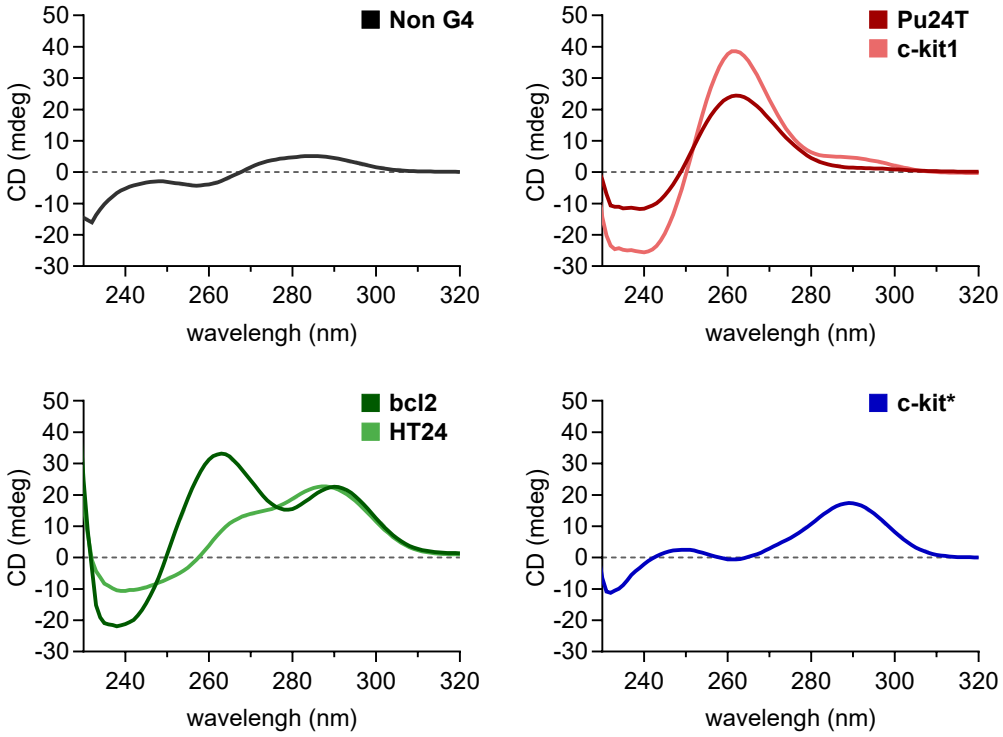

Supplementary Figure S3. Circular dichroism (CD) spectra of various oligonucleotides. Non-G4 (black: Non G4), parallel G4 (red: c-kit1, Pu24T), hybrid G4 (green: bcl2, HT24), and antiparallel G4 (blue: c-kit).

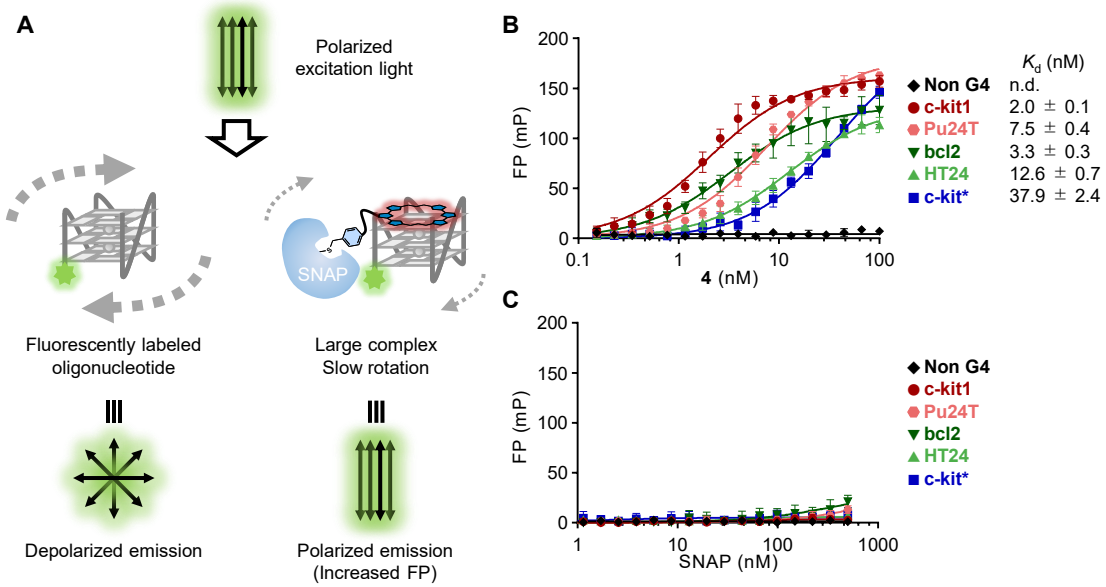

Supplementary Figure S4. Evaluation of G4-binding affinity of compound **4** using a fluorescence polarization (FP) assay. (A) Schematic representation of the FP assay. (B, C) Binding curves and dissociation constants (K_d) obtained from FP assays. The binding of compound **4** and SNAP-tag to non-G4-forming sequences (Non G4) and G4-forming sequences (c-kit1, Pu24T, bcl2, HT24, and c-kit*) was evaluated. Data represent the mean ± standard deviation (s.d.) from five independent experiments ($n = 5$).

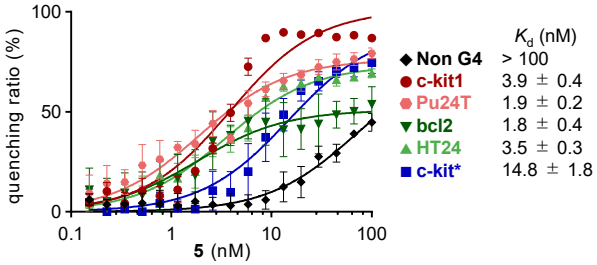

Supplementary Figure S5. Binding curves and dissociation constants (K_d) obtained from fluorescence quenching assays. The binding of compound **5** to non-G4-forming sequences (Non G4) and G4-forming sequences (c-kit1, Pu24T, bcl2, HT24, and c-kit*) was evaluated. Data represent the mean ± standard deviation (s.d.) from five independent experiments ($n = 5$).

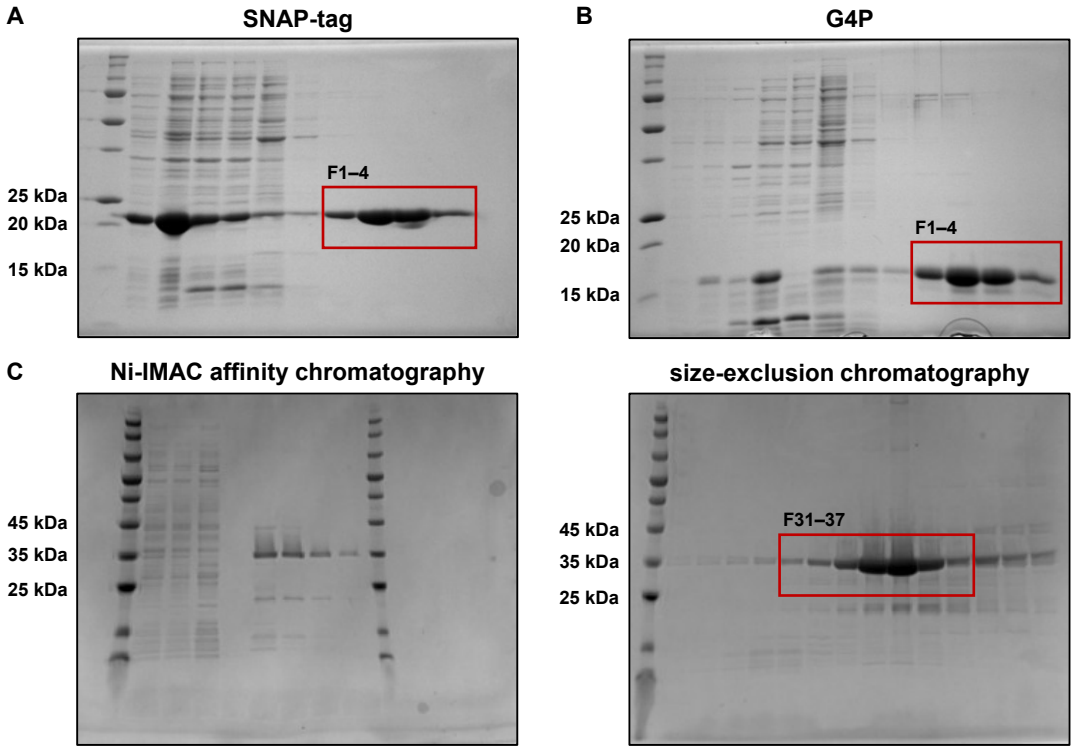

Supplementary Figure S6. SNAP-tag (A) and G4P (B) proteins were purified using Ni-NTA affinity chromatography. Fractions 1–4 were collected and subjected to dialysis to remove imidazole. The resulting proteins were concentrated and used in downstream assays. (C) BG4 was purified to apparent homogeneity by Ni-IMAC affinity chromatography (left), followed by further purification by size-exclusion chromatography (right). Fractions 31–37 were collected, concentrated, and used in downstream assays.

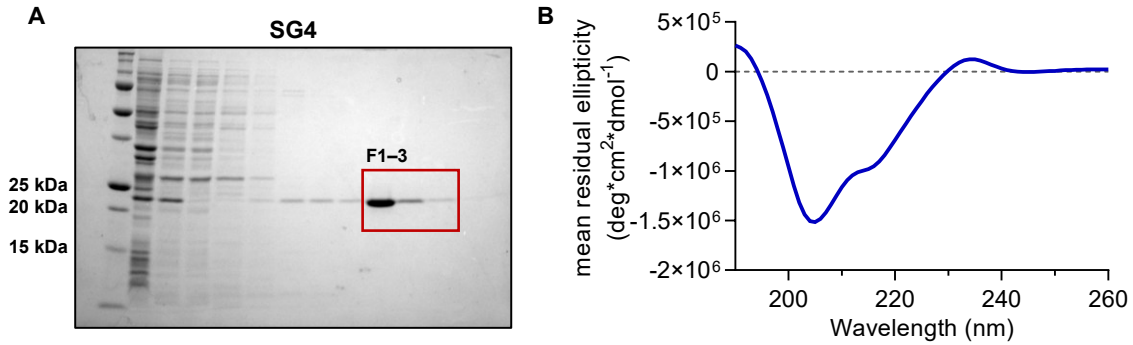

Supplementary Figure S7. (A) SG4 was purified using Ni-NTA affinity chromatography. Fractions 1–3 were collected and subjected to dialysis to remove imidazole. The resulting proteins were concentrated and used in downstream assays. (B) Secondary structure of SG4 as determined by CD spectroscopy (190–260 nm). A spectrum consistent with previous reports was obtained.[9]

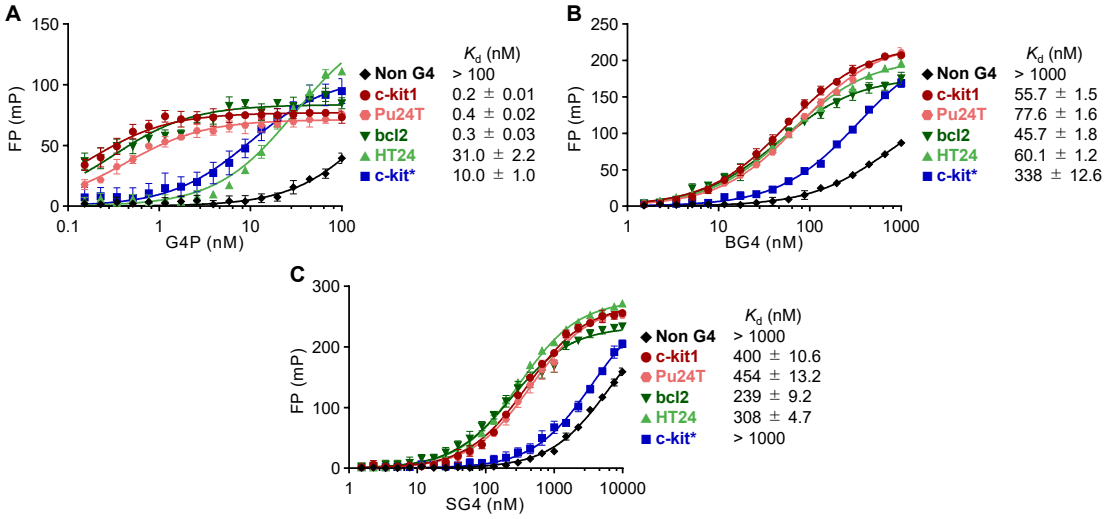

Supplementary Figure S8. Increase in fluorescence polarization (FP) induced by increasing concentrations of binary complexes of G4P (A), BG4 (B), or SG4 (C) with various G4 structures. FP was measured for binding to G4-forming sequences (c-kit1, Pu24T, bcl2, HT24, and c-kit*) and a non-G4-forming control (Non G4). Apparent dissociation constants (K_d) are shown. Data represent the mean ± standard deviation (s.d.) from five independent experiments ($n = 5$).

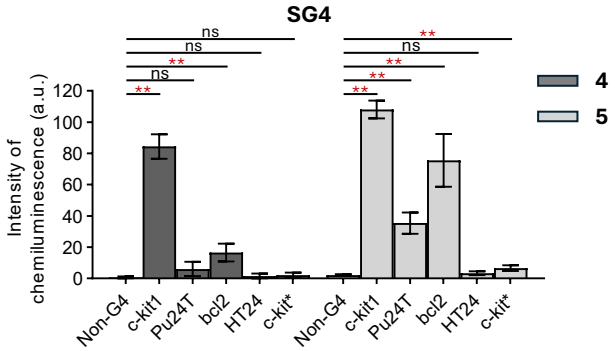

Supplementary Figure S9. Analysis of ternary complex formation of SG4 using the sandwich ELISA method. An increase in chemiluminescence indicates enhanced co-binding. Data represent the mean ± standard deviation (s.d.) from six independent experiments ($n = 6$). a.u., arbitrary units. Statistical analysis was performed using the Mann–Whitney U test (unpaired); $^{**}P < 0.01$.

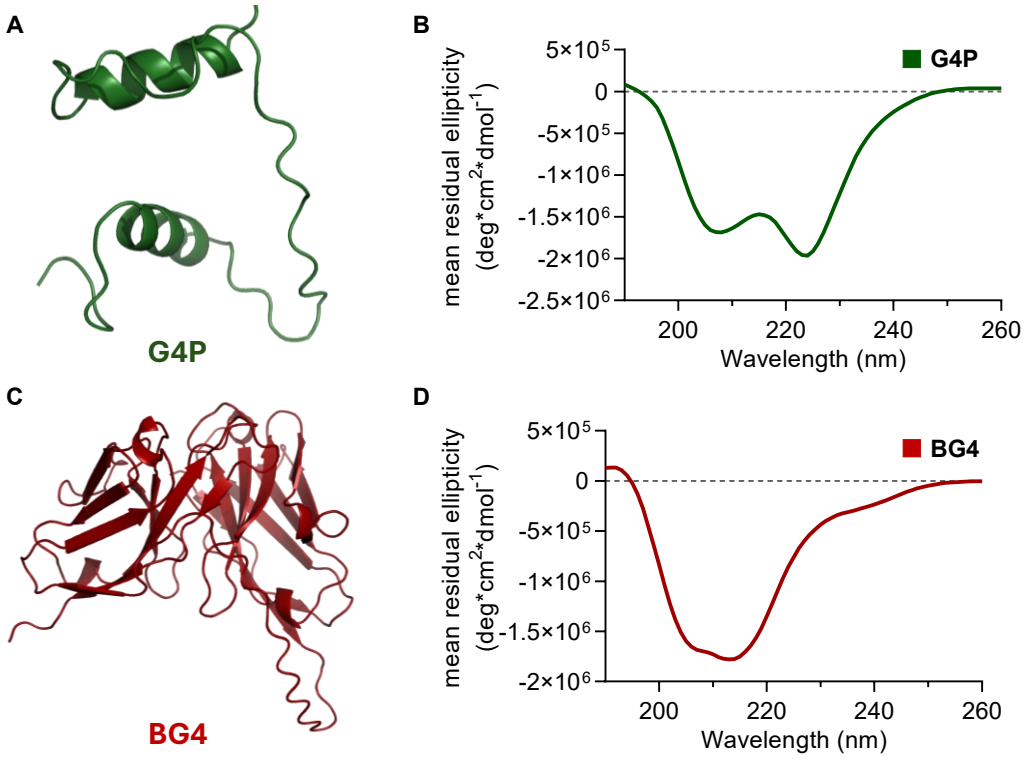

Supplementary Figure S10. (A) AlphaFold3-predicted structure of G4P.[10] (B) Secondary structure of G4P determined by CD spectroscopy (190–260 nm), showing a characteristic α-helix with negative peaks at 207 nm and 222 nm. (C) AlphaFold3-predicted structure of BG4. (D) Secondary structure of BG4 determined by CD spectroscopy (190–260 nm), showing a characteristic β-sheet with a broad negative peak between 217 and 230 nm.

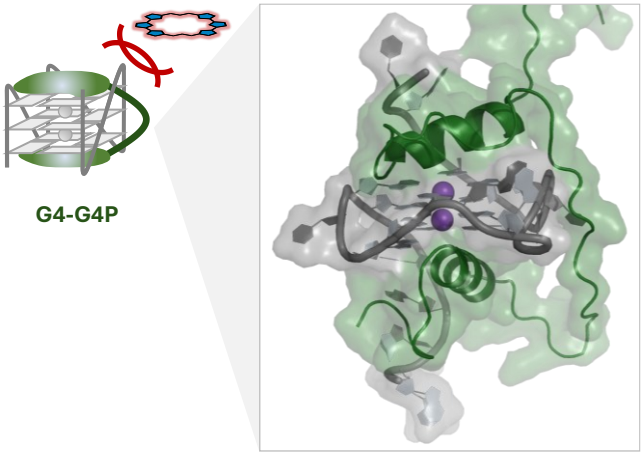

Supplementary Figure S11. Predicted complex structure of G4P and Pu24T generated by AlphaFold3.

Synthetic procedures

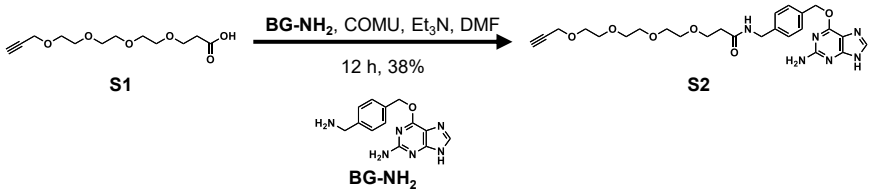

N-(4-(((2-amino-9H-purin-6-yl)oxy)methyl)benzyl)-4,7,10,13-tetraoxahexadec-15-ynamide (S4): **S3** was synthesized according to a previously reported procedure[11]. **S3** (100 mg, 0.38 mmol) was dissolved in 19 mL of dry DMF (20 mM), followed by the sequential addition of COMU (197 mg, 0.46 mmol) and triethylamine (59 µL, 0.42 mmol). The reaction mixture was stirred under argon at room temperature for 5 min, after which **BG-NH₂** (135 mg, 0.50 mmol) was added. The mixture was stirred at room temperature for 12 h. The solvent was removed in vacuo, and the residue was purified by silica gel column chromatography ($CHCl_3$/MeOH = 85/15) to give **S4** as a white solid (74.2 mg, 38%).

^{1}H-NMR (500 MHz, DMSO- d_6) δ 8.38 (t, J = 5.2 Hz, 1H), 7.85 (s, 1H), 7.45 (d, J = 6.9 Hz, 2H), 7.27 (d, J = 6.9 Hz, 2H), 6.32 (s, 2H), 5.46 (s, 2H), 4.28 (d, J = 5.7 Hz, 2H), 4.13 (t, J = 2.3 Hz, 2H), 3.63 (t, J = 5.7 Hz, 2H), 3.53-3.48 (m, 13H), 3.43 (d, J = 2.3 Hz, 1H), 2.38 (t, J = 5.4 Hz, 2H).

^{13}C-NMR (126 MHz, DMSO- d_6) δ 171.2, 170.2, 159.7, 159.5, 156.0, 139.4, 138.4, 135.2, 128.6, 127.3, 80.4, 77.2, 69.8, 69.7, 69.6, 69.5, 68.5, 66.9, 66.6, 57.5, 41.9, 40.4, 40.0, 39.9, 39.7, 39.5, 39.3, 39.2, 39.0, 36.2, 34.6.

HRMS (ESI) $[M+Na]^+$ calculated for $C_{25}H_{32}N_6Na_1O_6$: 535.2276, found: 535.2263 (-1.28 mDa).

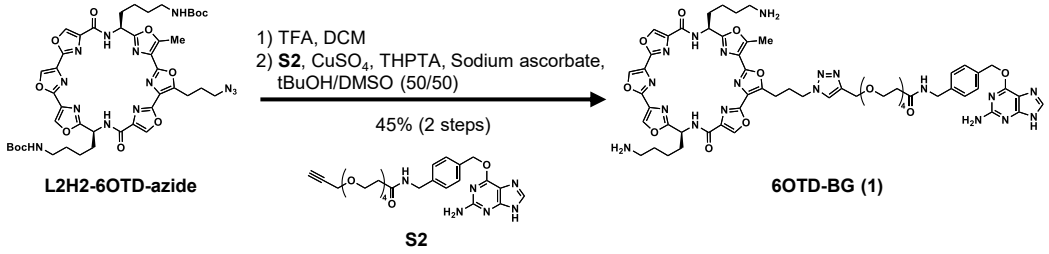

N-(4-(((2-amino-9H-purin-6-yl)oxy)methyl)benzyl)-1-(1-(3-((12Z,22Z,32Z,72Z,82Z,92Z,6S,12S)-6,12-bis(4-aminobutyl)-15-methyl-4,10-dioxo-5,11-diaza-1(2,4),2,3,7,8,9(4,2)-hexaoxazolacyclododecaphane-25-yl)propyl)-1H-1,2,3-triazol-4-yl)-2,5,8,11-tetraoxatetradecan-14-amide (6OTD-BG: 2): **L2H2-6OTD-azide** was synthesized according to a previously reported procedure[12]. To a solution of **L2H2-6OTD-azide** (37 mg, 0.039 mmol) was added DCM-TFA (10:1, 2.2 mL) at room temperature. The reaction mixture was stirred at room temperature for 12 h and then concentrated in vacuo to give the amine, which was used in the next step without further purification. The crude amine (18.6 mg, 0.019 mmol) was dissolved in tBuOH-DMSO (1:1, 0.4 ml, 47 mM) followed by the sequential addition of **S3** (9.7 mg, 0.0189 mmol), copper (II) Sulfate Pentahydrate (0.5 mg, 0.0019 mmol), THPTA (0.8 mg, 0.0019 mmol) and Sodium L-ascorbate (1.9 mg, 0.009 mmol). The reaction mixture was stirred at room temperature for 72 h. The residue was purified by reversed-phase chromatography to afford **6OTD-BG (2)** as a white solid (12.6 mg, 45%, 2 steps).

^{1}H-NMR (500 MHz, DMSO- d_6) δ 9.12 (d, J = 6.9 Hz, 2H), 8.93 (s, 1H), 8.79 (s, 1H), 8.37 (t, J = 5.7 Hz, 1H), 8.29 (dd, J = 12.6, 7.4 Hz, 2H), 8.11 (s, 1H), 7.80 (s, 5H), 7.43 (d, J = 8.0 Hz, 2H), 7.25 (d, J = 7.4 Hz, 3H), 7.17-7.14 (m, 2H), 6.28 (s, 2H), 5.44 (s, 3H), 5.36 (q, J = 5.9 Hz, 1H), 4.48 (s, 4H), 4.25 (d, J = 5.7 Hz, 2H), 3.60 (t, J = 6.3 Hz, 2H), 3.52-3.46 (m, 13H), 3.13 (t, J = 6.9 Hz, 2H), 2.75 (t, J = 6.3 Hz, 4H), 2.70 (s, 3H), 2.36 (d, J = 6.3 Hz, 4H), 2.06 (s, 2H), 1.92 (s, 2H), 1.48 (d, J = 54.4 Hz, 6H), 1.20 (s, 2H).

^{13}C-NMR (126 MHz, DMSO- d_6) δ 170.2, 164.4, 162.0, 159.7, 158.9, 158.8, 158.5, 158.2, 158.0, 157.7, 155.7, 155.4, 154.7, 154.6, 153.0, 151.7, 144.0, 142.6, 142.3, 141.8, 141.1, 139.4, 137.4,

136.0, 135.8, 135.2, 129.7, 128.9, 128.5, 128.2, 127.2, 125.4, 124.9, 123.9, 123.7, 69.8, 69.7, 69.7, 69.5, 69.0, 66.9, 66.6, 63.6, 48.5, 47.2, 47.1, 41.8, 40.0, 39.9, 39.9, 39.8, 39.7, 39.5, 39.4, 39.2, 39.0, 38.7, 36.1, 33.4, 27.6, 26.7, 22.4, 21.1, 20.9, 20.9, 11.6.
HRMS (ESI) $[M+2H]^{2+}$ calculated for $C_{59}H_{71}N_{19}O_{14}$: 634.7709, found: 634.7685 (-2.32 mDa). $[M+H]^{+}$ calculated for $C_{59}H_{70}N_{19}O_{14}$: 1268.5344, found: 1268.5326 (-1.83 mDa).

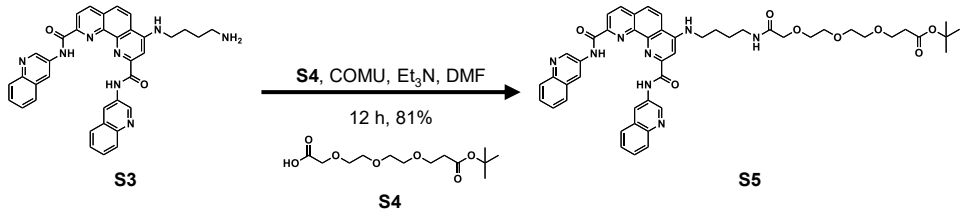

tert-butyl 17-((2,9-bis(quinolin-3-ylcarbamoyl)-1,10-phenanthrolin-4-yl)amino)-12-oxo-4,7,10-trioxa-13-azaheptadecanoate (S6): S1 and **S5** were synthesized according to a previously reported procedure[13,14]. **S1** (58 mg, 0.2 mmol) was dissolved in 3.3 mL of dry DMF (50 mM), followed by the sequential addition of COMU (85 mg, 0.2 mmol) and triethylamine (27 µL, 0.2 mmol). The reaction mixture was stirred under argon at room temperature for 5 min, after which **S5** (100 mg, 0.17 mmol) was added. The mixture was stirred at room temperature for 12 h. The solvent was removed in vacuo, and the residue was purified by silica gel column chromatography (NH Silica; $CHCl_3$/MeOH = 99/1) to give **S6** as a yellow solid (117 mg, 81%).
^{1}H-NMR (500 MHz, DMSO- d_6) δ 11.63 (d, J = 17.8 Hz, 2H), 9.62 (dd, J = 6.6, 2.0 Hz, 2H), 9.02 (dd, J = 16.0, 2.3 Hz, 2H), 8.62 (d, J = 8.0 Hz, 1H), 8.47 (d, J = 8.0 Hz, 1H), 8.41 (d, J = 9.2 Hz, 1H), 8.05 (t, J = 8.6 Hz, 3H), 8.00 (d, J = 7.4 Hz, 1H), 7.94 (d, J = 9.2 Hz, 1H), 7.78 (t, J = 5.7 Hz, 1H), 7.73-7.60 (m, 5H), 7.51 (s, 1H), 3.90 (s, 2H), 3.58-3.46 (m, 17H), 3.37 (q, J = 6.3 Hz, 2H), 3.24 (q, J = 6.5 Hz, 2H), 2.38 (t, J = 6.3 Hz, 2H), 1.76-1.71 (m, 2H), 1.65-1.59 (m, 2H), 1.34 (s, 9H).
^{13}C-NMR (126 MHz, DMSO- d_6) δ 170.4, 169.2, 164.0, 163.8, 163.4, 152.0, 149.4, 148.7, 145.4, 145.3, 144.6, 144.5, 144.1, 138.0, 132.5, 132.5, 130.3, 128.7, 128.2, 128.1, 128.0, 127.9, 127.1, 127.0, 124.5, 123.4, 123.1, 122.4, 120.9, 119.0, 99.1, 79.7, 70.3, 70.0, 69.7, 69.7, 69.6, 66.2, 65.9, 47.0, 42.6, 40.4, 40.0, 39.9, 39.7, 39.5, 39.4, 39.2, 39.0, 38.0, 37.9, 35.8, 27.7, 27.1, 25.2.
HRMS (ESI) $[M+H]^{+}$ calculated for $C_{49}H_{53}N_8O_8$: 881.3981, found: 881.3963 (-1.83 mDa).

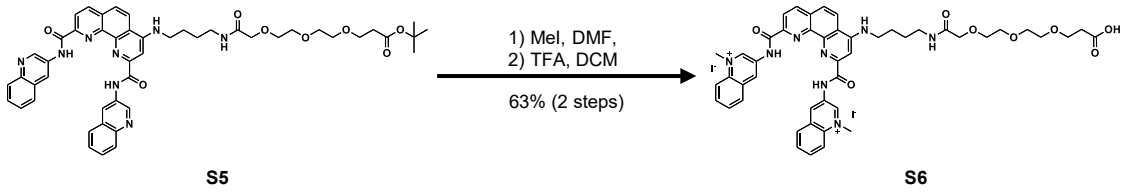

3,3'-((4-((1-carboxy-11-oxo-3,6,9-trioxa-12-azahexadecan-16-yl)amino)-1,10-phenanthroline-2,9-dicarbonyl)bis(azanediyl))bis(1-methylquinolin-1-ium) (S7): **S6** (234 mg, 0.27 mmol) was dissolved in 8.9 mL of dry DMF (30 mM) and heated to 40 °C before methyl iodide (1.7 mL, 26.6 mmol) was added dropwise. The reaction mixture was stirred under argon at 40 °C for 12 h and then concentrated in vacuo. The resulting crude product was used in the next step without further purification. The crude material was dissolved in DCM-TFA (10:1, 11 mL) at room temperature and stirred for 12 h. The solvent was removed in vacuo, and the residue was purified by reversed-phase chromatography to afford **S7** as a yellow solid (184 mg, 63%).
^{1}H-NMR (500 MHz, DMSO- d_6) δ 12.17 (s, 2H), 10.32 (s, 2H), 9.89 (s, 2H), 8.85 (d, J = 8.0 Hz, 1H), 8.67-8.47 (m, 6H), 8.23-8.17 (m, 3H), 8.06 (s, 3H), 7.82 (s, 1H), 7.67 (s, 1H), 4.73 (d, J = 5.7 Hz, 6H), 3.89 (s, 2H), 3.59-3.49 (m, 12H), 3.24 (d, J = 6.3 Hz, 2H), 2.43 (t, J = 5.7 Hz, 2H), 1.79 (t, J = 6.6 Hz, 2H), 1.66 (t, J = 6.9 Hz, 2H).
^{13}C-NMR (126 MHz, DMSO- d_6) δ 172.7, 169.3, 164.4, 163.8, 158.1, 157.9, 152.4, 148.0, 145.8, 138.8, 135.4, 134.7, 134.4, 133.9, 132.9, 130.9, 130.3, 129.9, 129.2, 125.2, 123.0, 121.6, 119.4,

119.2, 118.4, 116.0, 99.6, 70.3, 70.0, 69.7, 69.6, 69.6, 66.3, 46.1, 42.6, 40.0, 39.9, 39.7, 39.5, 39.3, 39.2, 39.0, 37.8, 34.8, 27.1, 25.2.
HRMS (ESI) $[M+2H]^{2+}$ calculated for $C_{47}H_{50}N_8O_8$: 427.1870, found: 427.1852 (-1.79 mDa). $[M+H]^+$ calculated for $C_{47}H_{49}N_8O_8$: 853.3668, found: 853.3635 (-3.29 mDa).

3,3'-((4-((1-(4-(((2-amino-9H-purin-6-yl)oxy)methyl)phenyl)-3,14-dioxo-6,9,12-trioxa-2,15-diazanonadecan-19-yl)amino)-1,10-phenanthroline-2,9-dicarbonyl)bis(azanediyl))bis(1-methylquinolin-1-ium) (PhenDC$_3$-BG: 3): **S7** (60 mg, 0.054 mmol) was dissolved in 2.7 mL of dry DMF (20 mM), followed by the sequential addition of COMU (25.5 mg, 0.06 mmol) and triethylamine (8.3 µL, 0.06 mmol). The reaction mixture was stirred at room temperature for 5 min, after which **BG-NH2** (29.3 mg, 0.11 mmol) was added. The mixture was stirred under argon at room temperature for 12 h. The solvent was removed in vacuo, and the residue was purified by reversed-phase chromatography to give **PhenDC$_3$-BG (3)** as a yellow solid (19.4 mg, 26%).

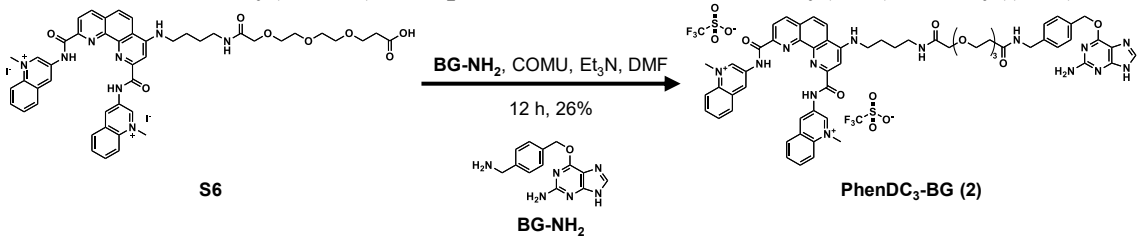

^{1}H-NMR (500 MHz, DMSO- d_6) δ 12.11 (d, J = 22.3 Hz, 2H), 10.30 (s, 2H), 9.89 (d, J = 6.9 Hz, 2H), 8.86 (d, J = 8.0 Hz, 1H), 8.68 (d, J = 8.0 Hz, 1H), 8.61-8.47 (m, 5H), 8.37 (s, 1H), 8.26-8.17 (m, 3H), 8.07 (q, J = 7.6 Hz, 2H), 7.97 (s, 1H), 7.83-7.78 (m, 2H), 7.69 (s, 1H), 7.42 (d, J = 6.9 Hz, 2H), 7.24 (d, J = 6.9 Hz, 2H), 6.30 (s, 2H), 5.42 (s, 2H), 4.72 (d, J = 9.7 Hz, 6H), 4.32-4.25 (m, 5H), 3.89 (s, 2H), 3.62-3.48 (m, 11H), 3.24 (q, J = 6.1 Hz, 2H), 2.36 (t, J = 5.7 Hz, 2H), 1.77 (d, J = 6.9 Hz, 2H), 1.65 (t, J = 7.2 Hz, 2H), 1.29-1.26 (m, 4H).
^{13}C-NMR (126 MHz, DMSO- d_6) δ 170.2, 169.3, 164.5, 163.8, 159.6, 158.8, 152.3, 148.6, 148.0, 145.8, 145.8, 144.8, 144.3, 139.4, 138.8, 135.5, 135.4, 135.2, 134.7, 134.5, 133.9, 133.8, 132.9, 131.0, 130.3, 130.3, 130.0, 129.9, 129.2, 128.5, 127.2, 125.9, 125.3, 123.0, 122.0, 121.6, 119.5, 119.4, 119.2, 109.2, 99.6, 70.3, 70.0, 69.7, 69.6, 66.9, 66.6, 62.4, 46.0, 46.0, 42.6, 41.8, 40.0, 39.9, 39.9, 39.8, 39.7, 39.5, 39.4, 39.2, 39.0, 37.8, 36.1, 27.1, 25.2, 13.9.
HRMS (ESI) $[M+2H]^{2+}$ calculated for $C_{60}H_{62}N_{14}O_8$: 553.2432, found: 553.2419 (-1.29 mDa). $[M+H]^+$ calculated for $C_{60}H_{61}N_{14}O_8$: 1105.4791, found: 1105.4777 (-1.42 mDa).

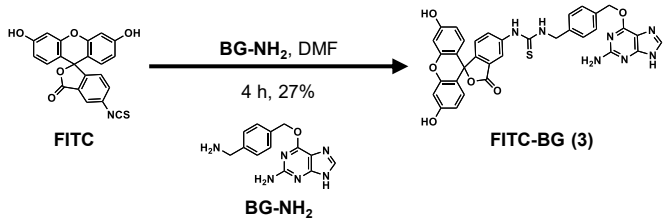

1-(4-(((2-amino-9H-purin-6-yl)oxy)methyl)benzyl)-3-(3',6'-dihydroxy-3-oxo-3H-spiro[isobenzofuran-1,9'-xanthen]-5-yl)thiourea (FITC-BG: 4): **FITC** (30 mg, 0.077 mmol) was dissolved in 10 mL of dry DMF (7.7 mM), followed by the addition of **BG-NH$_2$** (28.4 mg, 0.11 mmol). The reaction mixture was stirred under argon at room temperature for 4 h. The solvent was removed in vacuo, and the residue was purified by reversed-phase chromatography to afford **FITC-BG (4)** as a dark brown solid.
^{1}H-NMR (500 MHz, DMSO- d_6) δ 12.43 (s, 1H), 10.10 (d, J = 48.7 Hz, 3H), 8.52 (s, 1H), 8.25 (s, 1H), 7.81-7.75 (m, 2H), 7.50 (d, J = 8.0 Hz, 2H), 7.39 (d, J = 8.0 Hz, 2H), 7.19 (d, J = 8.0 Hz, 1H), 6.67-6.55 (m, 7H), 6.32 (s, 2H), 5.47 (s, 2H), 4.80 (s, 2H).
HRMS (ESI) $[M+H]^+$ calculated for $C_{52}H_{67}N_8O_{11}S$: 660.1660, found: 660.1639 (-2.04 mDa).

NMR spectra

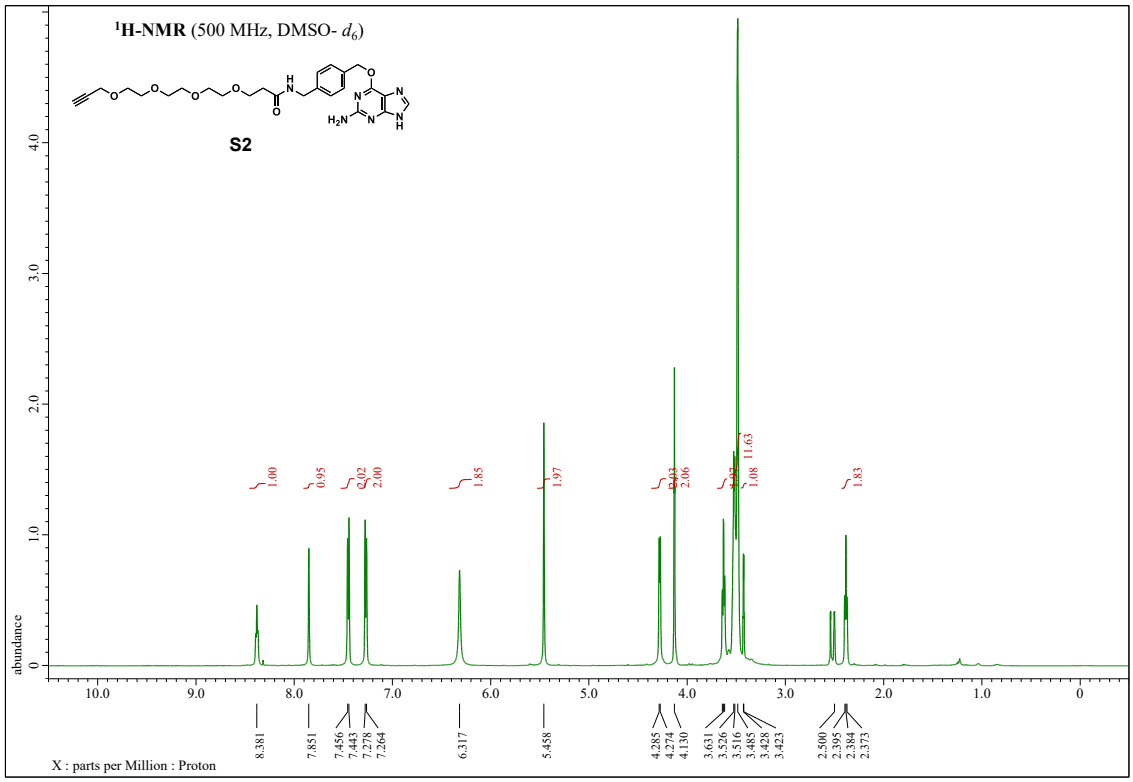
^{1}H-NMR (500 MHz, DMSO- d_6)
S2
abundance
X : parts per Million : Proton

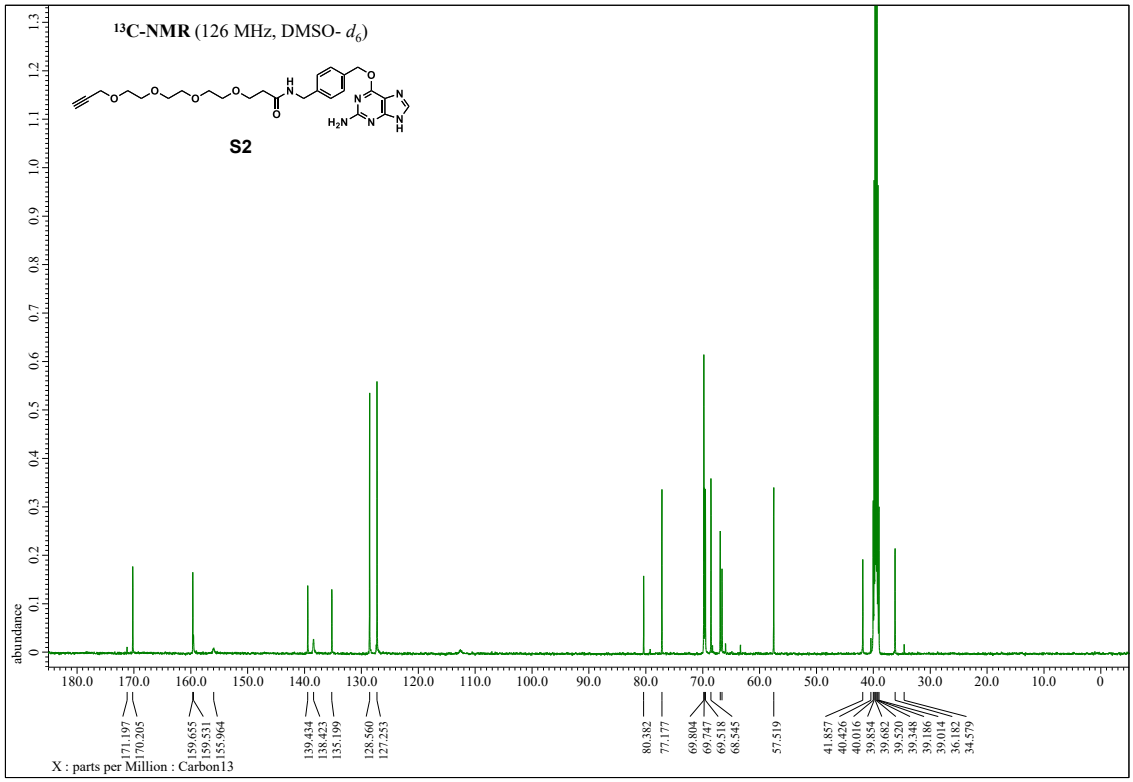
^{13}C-NMR (126 MHz, DMSO- d_6)
S2
abundance
X : parts per Million : Carbon13

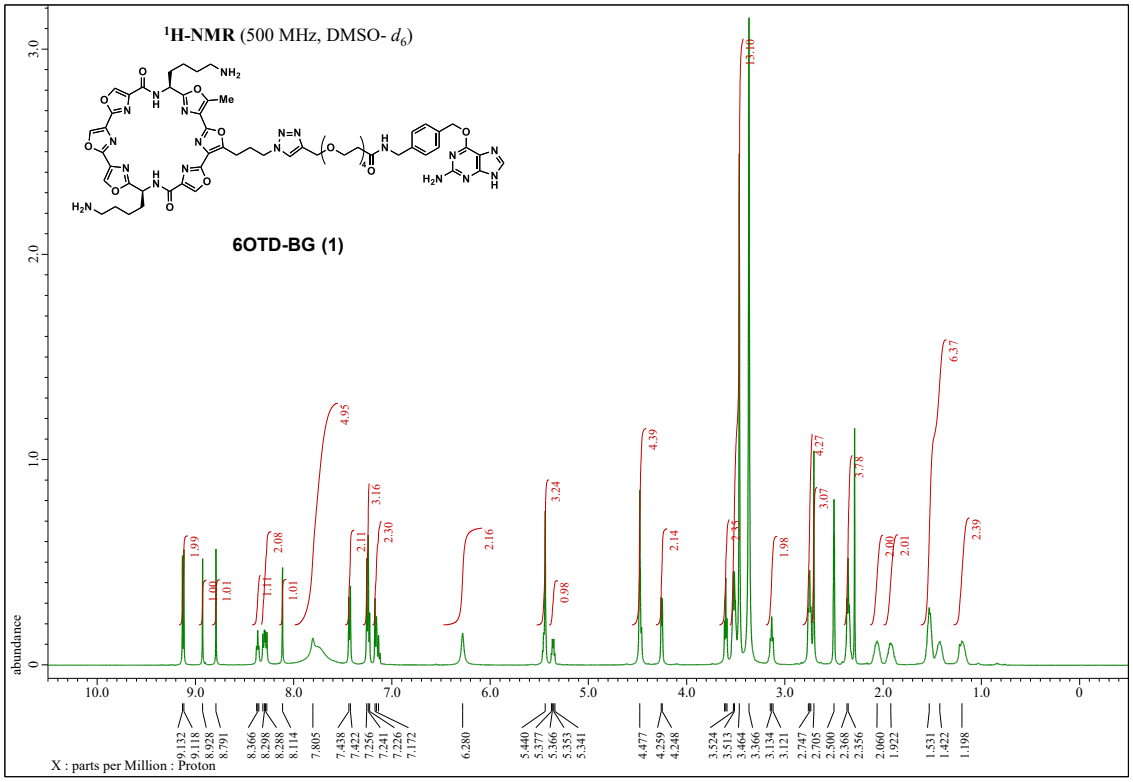
^{1}H-NMR (500 MHz, DMSO- d_6)
6OTD-BG (1)
abundance
X : parts per Million : Proton

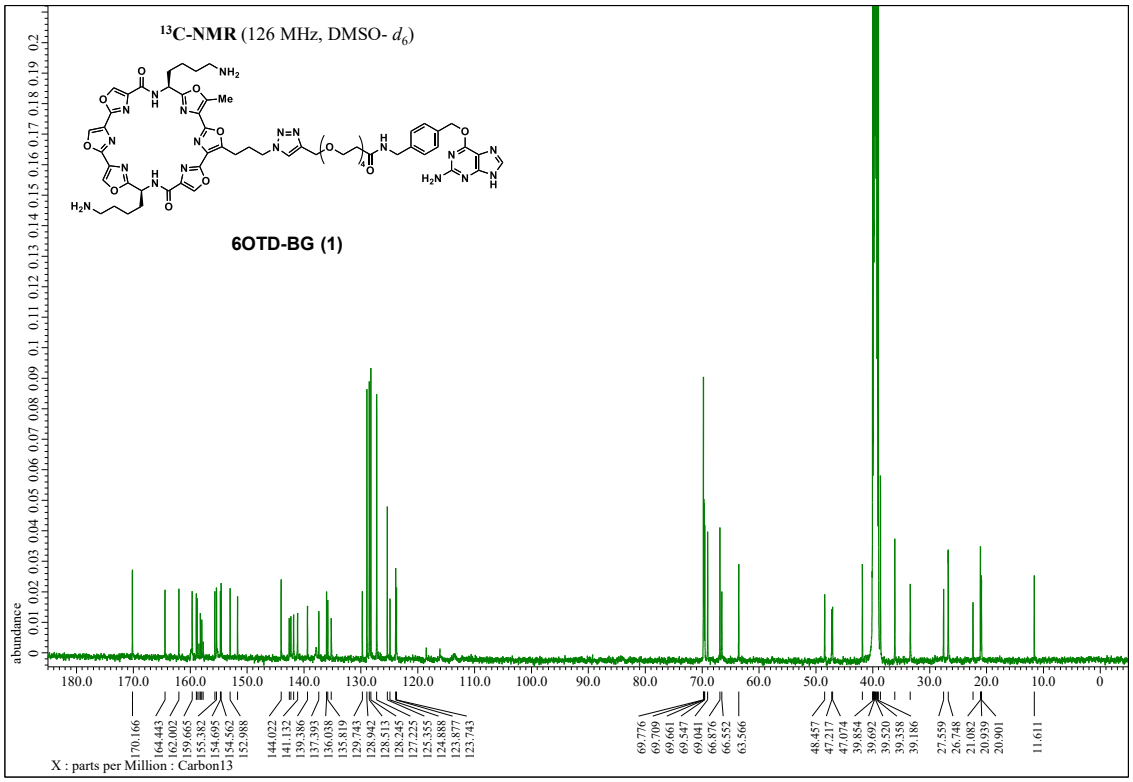
^{13}C-NMR (126 MHz, DMSO- d_6)
6OTD-BG (1)
abundance
X : parts per Million : Carbon13

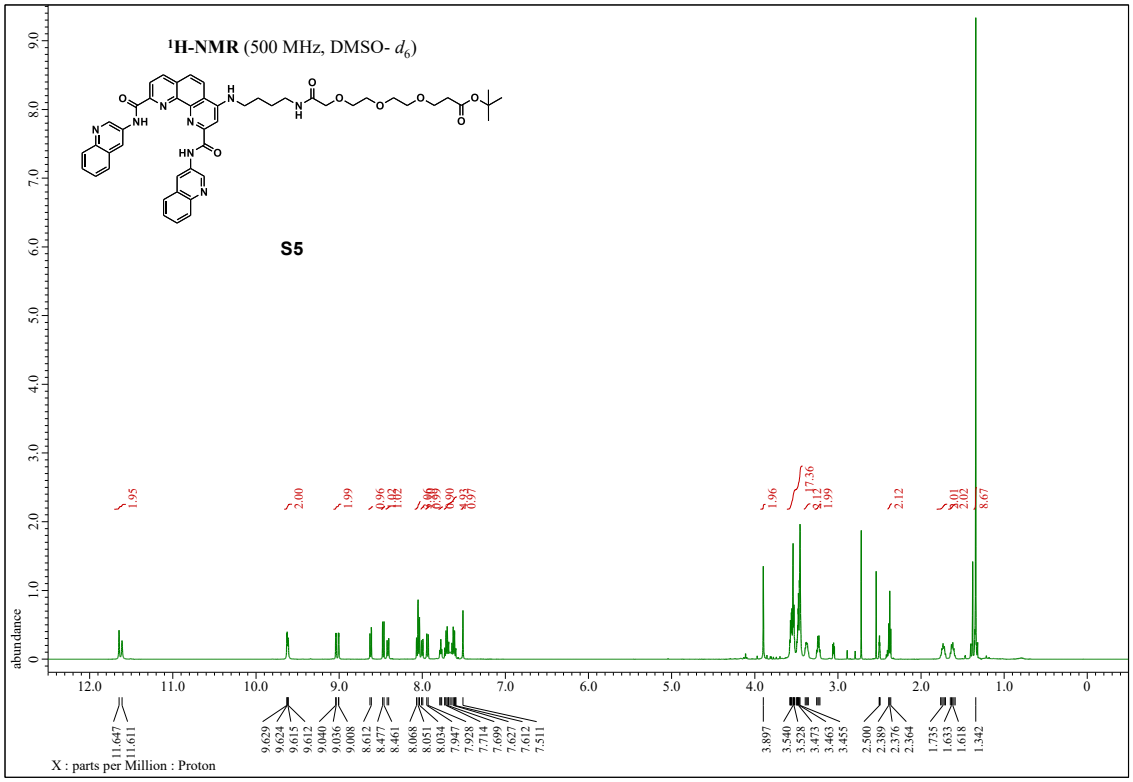
¹H-NMR (500 MHz, DMSO- d_6)
S5
abundance
X : parts per Million : Proton

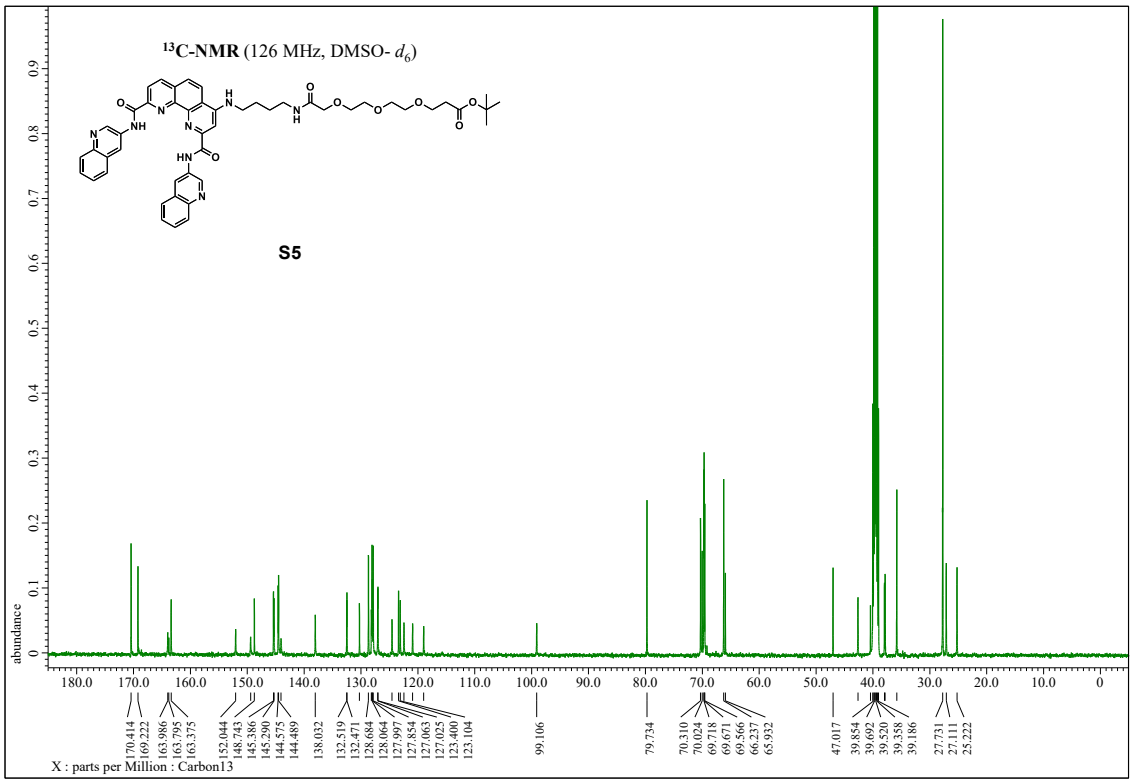
¹³C-NMR (126 MHz, DMSO- d_6)
S5
abundance
X : parts per Million : Carbon13

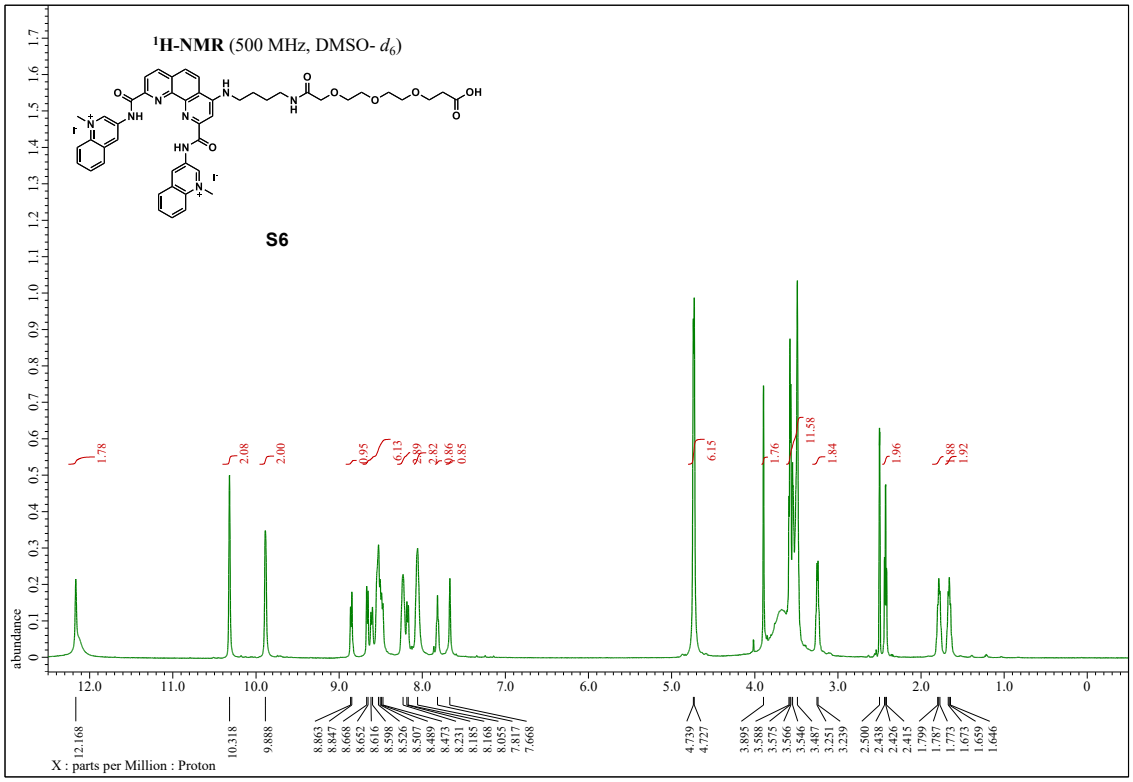
¹H-NMR (500 MHz, DMSO- d_6)
S6
abundance
X : parts per Million : Proton

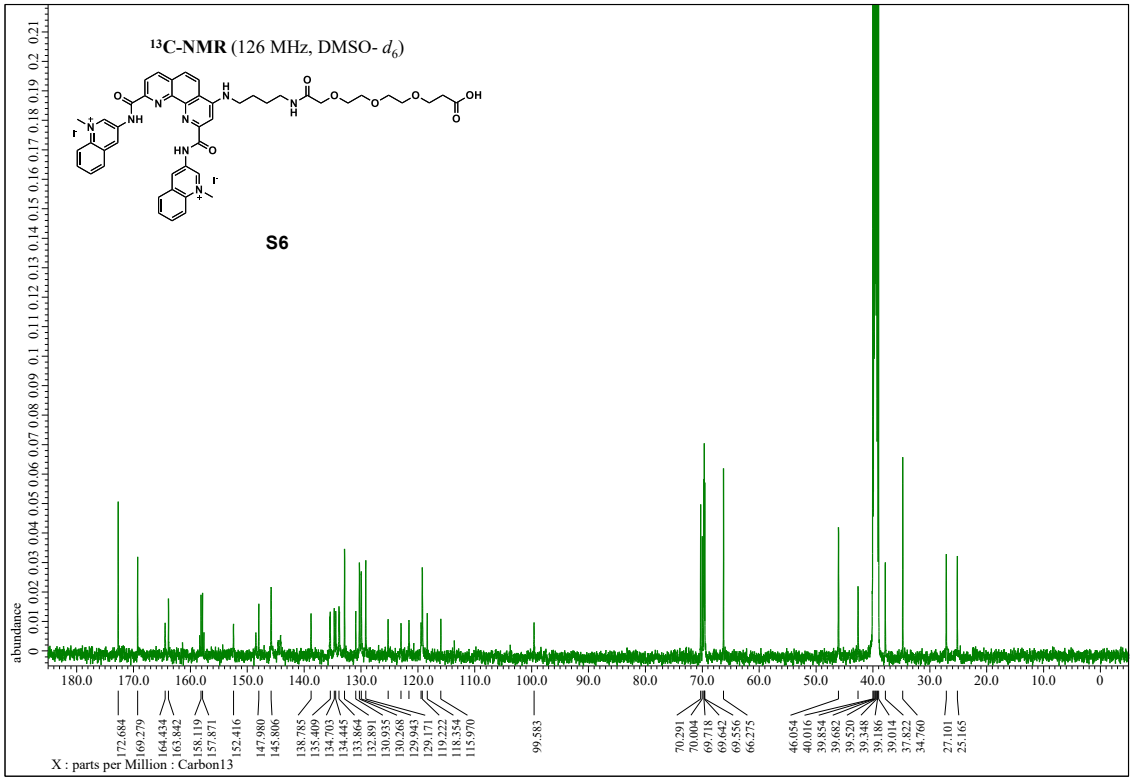
¹³C-NMR (126 MHz, DMSO- d_6)
S6
abundance
X : parts per Million : Carbon13

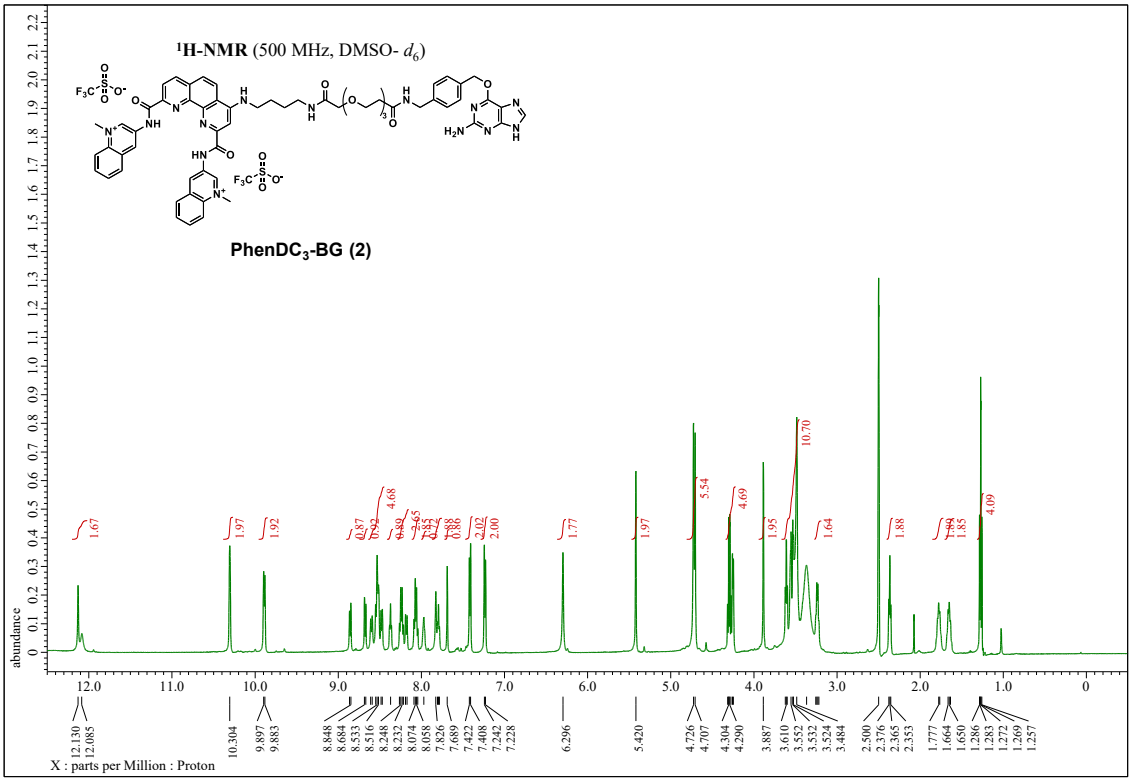
¹H-NMR (500 MHz, DMSO- d_6)
PhenDC$_3$-BG (2)
abundance
X : parts per Million : Proton

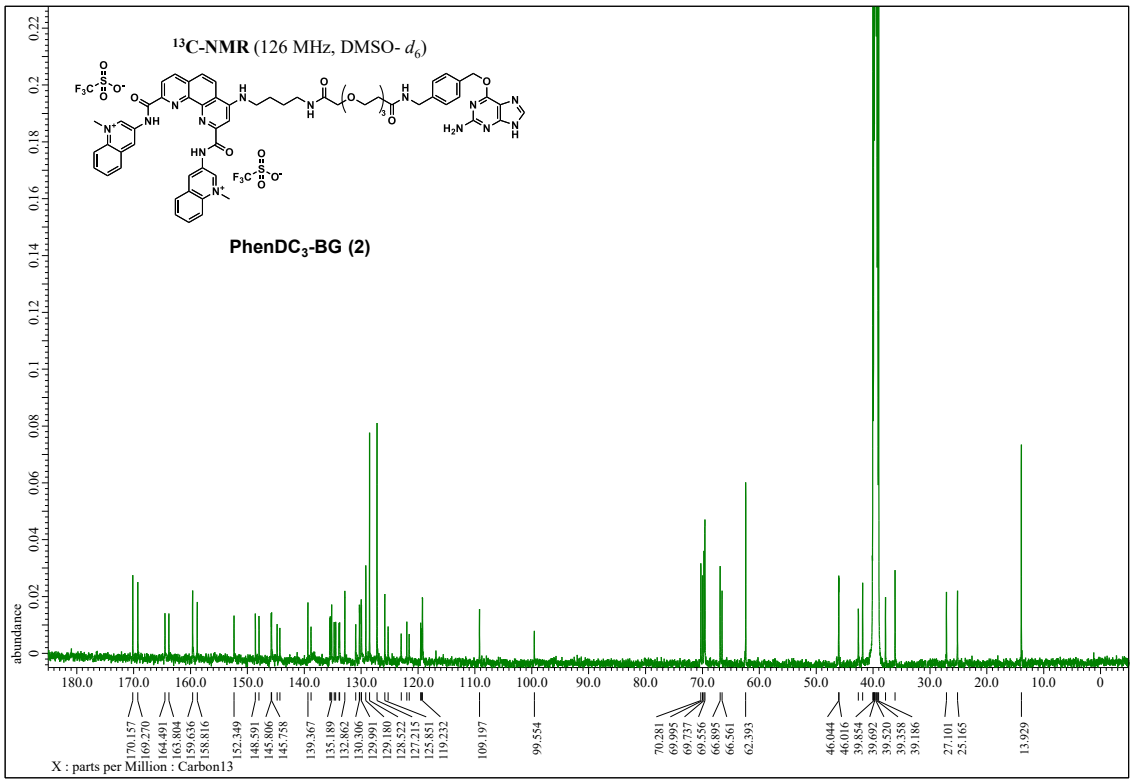
¹³C-NMR (126 MHz, DMSO- d_6)
PhenDC$_3$-BG (2)
abundance
X : parts per Million : Carbon13

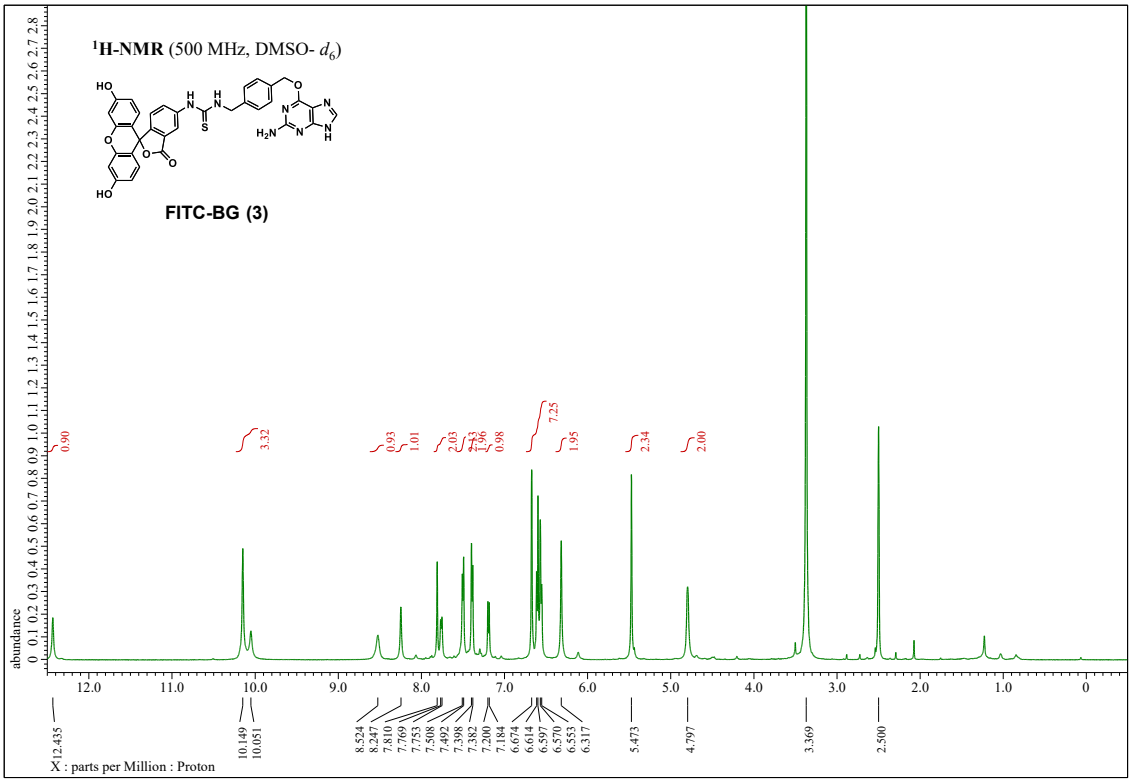

References

1 R. Asano, T. Kumagai, K. Nagai, S. Taki, I. Shimomura, K. Arai, H. Ogata, M. Okada, F. Hayasaka, H. Sanada, T. Nakanishi, T. Karvonen, H. Hayashi, Y. Katayose, M. Unno, T. Kudo, M. Umetsu & I. Kumagai, *Protein Eng. Des. Sel.*, 2013, **26**, 359–367.

2 D. Miura, H. Kimura, W. Tsugawa, K. Ikebukuro, K. Sode & R. Asano, *Talanta*, 2021, **234**, 122638.

3 F.W. Studier, *Protein Expr. Purif.*, 2005, **41**, 207–234.

4 T.T. Zhang, Z.T. Huang, Y. Dai, X.P. Chen, P. Zhu & G.H. Du, *Acta Pharmacol Sin*, 2006, **27**, 447–52.

5 J.H. Zhang, T.D. Chung & K.R. Oldenburg, *J Biomol Screen*, 1999, **4**, 67–73.

6 D. Li, Q. Han, X.Y. Yang, D.M. Rong & Z.J. Lin, *Acta Pharmacol Sin*, 1994, **15**, 211–4.

7 S.M. Kelly, T.J. Jess & N.C. Price, *Biochim. Biophys. Acta, Proteins Proteomics*, 2005, **1751**, 2, 119−139.

8 H.J. Motulsky & R.E. Brown, *BMC Bioinformatics*, 2006, **7**, 123.

9 S. Galli, L. Melidis, S.M. Flynn, D. Varshney, A. Simeone, J. Spiegel, S.K. Madden, D. Tannahill & S. Balasubramanian, *J. Am. Chem. Soc.*, 2022, **144**, 50, 23096–23103.

10 J. Abramson, J. Adler, J. Dunger, et al., *Nature*, 2024, **630**, 493–500.

11 V. Maggi, F. Bianchini, E. Portioli, S. Peppicelli, M. Lulli, D. Bani, R.D. Sole, F. Zanardi, A. Sartori & R. Fiammengo, *Chem. Eur. J.*, 2018, **24**, 12093.

12 J.A. Punnoose, Y. Ma, M.E. Hoque, Y. Cui, S. Sasaki, A.H. Guo, K. Nagasawa & H. Mao, *Biochemistry*, 2018, **57**, 51, 6946–6955.

13 E. Marini, M. Marino, G. Gionfriddo, F. Maione, M. Pandini, D. Oddo, M. Giorgis, B. Rolando, F. Blua, S. Gastaldi, S. Marchiò, S. Kovachka, F. Spyrakis, E. Gianquinto, F.D. Nicolantonio & M. Bertinaria, *Molecules*, 2022, **27**, 23, 8513.

14 J. Lefebvre, C. Guetta, F. Poyer, F. Mahuteau-Betzer & M.P. Teulade-Fichou, *Angew. Chem. Int. Ed.*, 2017, **56**, 11365.